Mechanical Properties and Crystallization Behavior of High Fluidity Polypropylene/Metallocene Poly(ethylene–butene–hexene) Copolymer Blends

Yingying Tang,[1][†] Jingyi Wang,[1] Hongbing Jia,[1] Lifeng Ding,[2] Qi Jiang[1]

[1]Key Laboratory for Soft Chemistry and Functional Materials of Ministry of Education, Nanjing University of Science and Technology, Nanjing, 210094, People's Republic of China
[2]Department of Chemical Engineering, University of Surrey, Guildford, GU2 7XH, UK
Yingying Tang and Jingyi Wang contributed equally to this work.
Correspondence to: H. Jia (E - mail: polymernjust@gmail.com)

ABSTRACT: This article presents a study on blends of high fluid polypropylene (HF-PP)/metallocene poly(ethylene–butane–hexene) copolymer (mEBHC) prepared by melt-blending process using a twin-screw extruder. Six different mass fractions of mEBHC in the blends: 0, 5, 10, 30%, and 100% were investigated in our study. The thermal behavior, fracture surface morphology, mechanical properties, and rheological properties of the blends were analyzed. Our results suggested that phase separation of HF-PP/mEBHC blends occurred during the cooling process. The addition of 30 wt % mEBHC resulted in a rise of crystallinity of HF-PP/mEBHC blends from 22.8% to 34.9%. The wide-angle X-ray diffraction (WAXD) showed that the incorporation of mEBHC did not have any influence on the intrinsic crystal structure of HF-PP. The droplet-matrix micrographs of the blends given by scanning electron microscope (SEM) revealed that mEBHC particles were dispersed as "droplet" in HF-PP continuous phase. When mEBHC content was increased up to 30%, the impact strength at 23°C and −20°C of HF-PP/mEBHC blends were improved by 150 and 35%, respectively, while the tensile strength and flexural strength were decreased slightly, compared to pristine HF-PP. The apparent shear viscosities of blends were similar to that of pristine HF-PP. © 2013 Wiley Periodicals, Inc. J. Appl. Polym. Sci. 130: 2557–2562, 2013

INTRODUCTION

Polypropylene (PP) is one of the most important engineering materials with excellent thermal and mechanical properties.[1–3] And, it has been used extensively in industry and domestic products, such as automobiles, electronic appliances, vessels and tube, spinning, and film.[4–7] In polymer processing, especially in the injection molding of large parts and automobile bumpers, high fluidity of PP's melt is favored.[8] Currently, there are two approaches to improve the fluidity of PP, namely controlled-rheology (CR) techniques[9] and novel catalyst with hydrogen modulation.[10] Compared with CR-PP, high-fluidity PP (HF-PP) produced by hydrogen modulation method is more transparent. And, no volatile organic compounds are involved.[11] However, high notch sensitivity and poor impact resistance of HF-PP[12] have limited its applications as an engineering plastic, especially under severe conditions.

Recently, metallocene catalytic polymerization of polyolefin copolymers, such as metallocene ethylene–octene copolymer (mEOc), metallocene propylene–1-octene copolymer (mPPOc) and metallocene liner low density polyethylene (mLLDPE) have been widely used as toughening agents for PP and PE,[2,3,13–19] which are mainly owning to their narrow molecular weight distribution, co-monomer distribution, and excellent physical and mechanical properties. McNally et al.[13] explored the toughing efficiency of mEOc on PP through mechanical blending and injection molding. They found that mEOc could significantly improve the impact strength of PP both at room temperature and cold temperature with 20∼30 wt % mEOc content. Wang et al.[17] synthesized iPP/mPPOc alloy through one-step polymerization process and found that notched Izod impact strength of iPP at room temperature was improved by 400% by adding 40 wt % mPPOc. Kukaleva et al.[19] studied the effect of mLLDPE content on the impact strength of "high-crystallinity" polypropylene (hcr-PP)

and found that the improved impact strength of blends reached maximum (17-fold) when mLLDPE content was up to 40%.

Metallocene poly (ethylene–butene–hexene) copolymer (mEBHC) is a novel metallocene catalytic polymerization of polyolefin copolymer with high melt flow rate. Compared to the conventional toughening agents, such as ethylene propylene rubber (EPR) or ethylene propylene diene monomer (EPDM), mEBHC exhibits the advantage of high melt flow properties. It has a much smaller viscosity difference with HF-PP. To the best of our knowledge, there has not been any research about the metallocene catalyzed polyolefin toughed HF-PP in the literature. In this article, mEBHC toughened HF-PP blends were prepared and studied with different contents of mEBHC through mechanical blending and then injection molding. The effects of mEBHC on the mechanical properties, crystallization behavior, rheological properties and the thermal behavior of HF-PP were investigated.

EXPERIMENTAL

Materials

HF-PP (YJP422, Sinopec-Yangzi Petro Co., Nanjing, China) with the melt flow rate (MFR) of 22 g/10 min (ASTMD1238, 230°C and 2.16 kg) was used as the matrix polymer. mEBHC ($\bar{M}_w$ = 54844, $\bar{M}_n$ = 19583, $\bar{M}_w/\bar{M}_n$ = 2.8, ρ = 0.919 g/cm³, MFR = 22 g/10 min (190°C and 2.16 kg) was synthesized (Sinopec-Qilu Petro Co., Shangdong, China) with the degree of branching (CH_3/10000C) of 17.1.

Sample Preparation

HF-PP and mEBHC were dried at 80°C for 24 h and then mixed by a high-speed mixing machine (model CH-10DY) for 10 min. Melt blending was performed using a twin-screw extruder (TE-35, Gelan Machinery Co., Zhangjiagang, China) with a rotation speed of 200 rpm. The temperature along the barrel was increased from 175 to 210°C: 175°C, 190°C, 190°C, 195°C, 200°C, and 210°C, respectively. The blends were cooled down before they were pelletized. The obtained blend pellets were dried again at 80°C in a vacuum oven before the injection molding and then were molded into standard sample by injection-machine (JN55-E, Chen Hsong Machinery Co., Ningbo, China). The mass fraction of mEBHC in blends was 0, 5, 10, 20, 30, and 100 wt %, and the weight ratios of HF-PP/mEBHC were designated as 100/0, 95/5, 90/10, 80/20, 70/30, and 0/100, respectively.

Mechanical Properties Tests

The V-notched Izod impact strength was determined by impact testing machine (ZBC1400-2, MTS systems corporation, Shenzhen, China) according to ASTM D256A. The tensile tests were evaluated using an electronic tensile tester (CMT4254, MTS systems corporation, Shenzhen, China) according to ASTM D638. The cross-head speed was 50 mm/min. Flexural tests were carried out according to ASTM D790A for materials using CMT4254 testing machine with cross-head speed of 10 mm/min.

Morphological Observation

A model JSM-6380LV JEOL scanning electron microscope (SEM) was used to observe the fracture surfaces of V-notched impact tests. The samples were sputter-coated with gold in a vacuum chamber.

Differential Scanning Calorimetry (DSC)

The thermal behavior of HF-PP and HF-PP/mEBHC blends were analyzed using a Mettler Toledo 823E Differential scanning calorimeter under nitrogen atmosphere. Approximately 5 mg samples were placed in aluminum pans and tested at a temperature range of 20–200°C. Samples were heated to 200°C with a heating rate of 10°C/min and kept for 5 min to erase thermomechanical histories. Then they were cooled to 20°C at a rate of 10°C/min and were then reheated up to 200°C at a rate of 10°C/min to determine the crystallization and melting temperatures. The degree of crystallization (X_c) is carried out as follows[20]:

$$X_c = \frac{\Delta H_{PP}^0}{\Delta H_{PP}^0 w} \times 100\%$$

where ΔH_{PP} is the melting enthalpies of PP in blends; ΔH_{PP}^0 is the standard melting enthalpies of PP (209 J/g),[21] and w is the mass fracture of PP in the blends.

Wide-Angle X-ray Diffraction (WAXD) Measurements

WAXD experiments were conducted on a Bruker D8 ADVANCE diffractometer (Cu $K\alpha$, λ = 0.154 nm, 40 kV, 30 mA) with 2θ at a range of 10–30°. The samples were cut from the injection molding samples.

Rheological Properties Tests

The flow properties of the blends were measured by a Rosand dual capillary rheometer (model RH2000) with a capillary/ die having a 0.5 mm diameter and length of 25 mm. Data were collected for all blends in the shear rate range 300–5000 s⁻¹ at 180, 200, and 220°C, respectively.

RESULTS AND DISCCUSSION

Thermal Behavior

Figure 1 shows the DSC thermograms of melting and crystallization curves of HF-PP/mEBHC blends at a heating and cooling rate of 10°C/min. It is obvious that blends of HF-PP/mEBHC-95/5, 90/10, 80/20, and 70/30 have two distinct peaks (one major peak and one minor peak) both in melting and cooling curves, indicating the presence of two different phase domains. During the cooling process, HF-PP and mEBHC chain segments in the melt tend to form their individual rich domains.[22] The melting and crystallization temperatures differences between HF-PP and mEBHC domain lead to liquid–liquid and solid–liquid phase separations. As a result, dual peaks of HF-PP/mEBHC blends were observed in the cooling process.

Figure 2 shows the composition dependence of melting and crystallization temperature of HF-PP/mEBHC blends. The melting and crystallization peak values of HF-PP gradually decrease with the increase of the incorporated mEBHC content, while the melting peak values of mEBHC gradually increase. In contrast to melting and crystallization temperatures of individual components, the shifts in the melting and crystallization peaks of the HF-PP/ mEBHC blends are caused by the kinetic effects or the thermal perturbations in the crystallization process, according to Ref. 23.

The X_c of HF-PP/mEBHC increases with the addition of mEBHC, which indicates that the mEBHC should act as a nucleation agent, which aids more crystallization of HF-PP (Table I). The flexible polymer blocks of mEBHC (including butene
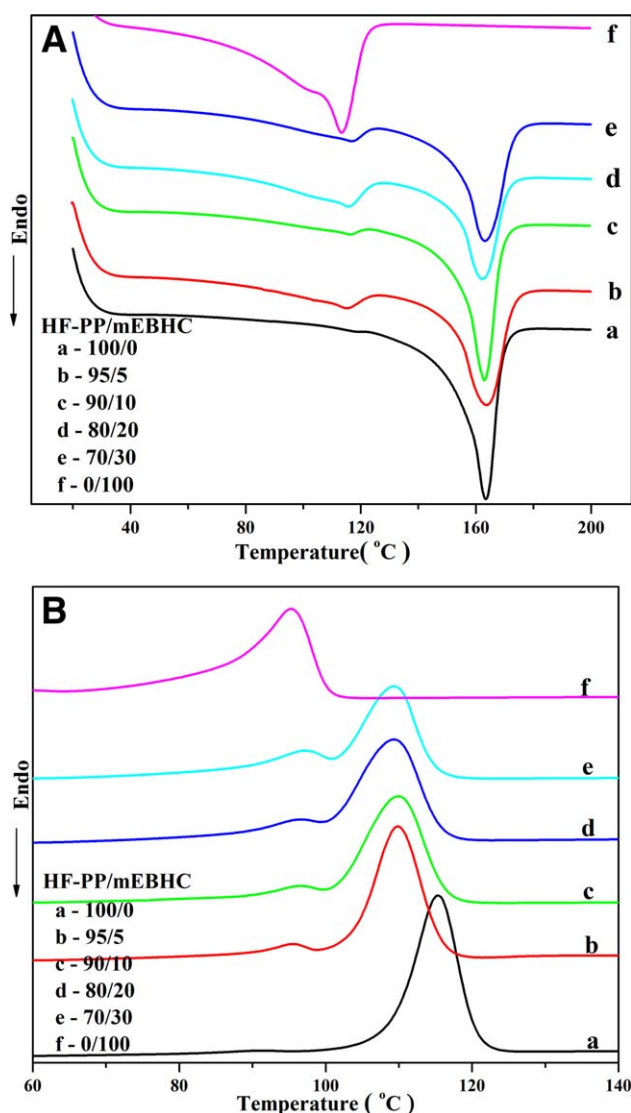
Figure 1. DSC thermograms of melting and crystallization curves for HF-PP/mEBHC blends: (a) melting curves; (b) crystallization curves. [Color figure can be viewed in the online issue, which is available at wileyonlinelibrary.com.]

and hexene segments) have high affinity with the macromolecule chains of HF-PP. Thus, when the butene and hexene segments of mEBHC move into HF-PP macromolecules, they may easily aggregate with HF-PP chains to form micelles, which act as nuclei for the HF-PP macromolecule segments to crystallize.[2]

WAXD Analysis. Figure 3 gives the WAXD diffractograms of HF-PP/mEBHC blends. For pristine HF-PP (curve a), there are four diffraction peaks at 13.9°, 16.7°, 18.3°, and 21.3°, which are characterized as α-crystal of PP and corresponded to the reflection planes at (1 1 0), (0 4 0), (1 3 0), and (1 1 1) respectively.[24,25] For pristine mEBHC (curve f), the diffractogram exhibits major characteristic crystalline peaks of PE at the scattering angles $2\theta = 21.5°$ and 23.8°, which correspond to the reflection planes at (1 1 0) and (2 0 0), respectively.[26] Apparently, the diffractograms of HF-PP/mEBHC blends (curve b, c, d, and e) still exhibit major characteristic crystalline peaks of
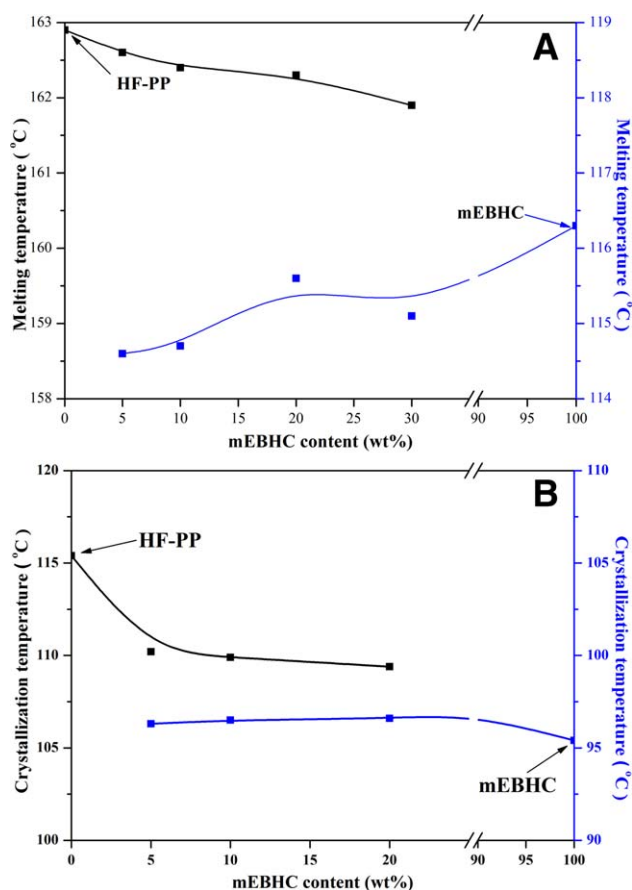

Figure 2. The composition dependence of melting and crystallization temperature of HF-PP/mEBHC blends (a): melting process; (b): cooling process. [Color figure can be viewed in the online issue, which is available at wileyonlinelibrary.com.]

HF-PP. It indicates that the intrinsic crystalline structure of HF-PP matrix is retained with the presence of incorporated mEBHC. The intensity and profile of the corresponding diffraction peaks of the blends however have been changed to some extent. The diffraction intensity of (0 4 0) and (1 1 0) decrease, while the intensity of (1 1 1) diffraction increase. $I_{(110)}$ and $I_{(040)}$ are the integrated intensity under crystalline peaks of PP. And they correspond to the reflection planes at (1 1 0) and (0 4 0) respectively. The ratio of $I_{(110)}$ and $I_{(040)}$ provides information on the relationship between orientation of a-axis and b-axis of α-crystal.[27] In Table II, the values of $I_{(110)}/I_{(040)}$ decrease with the addition of mEBHC, indicating that crystals grow along the b-axis preferentially.[8] Perfection of α-PP can be

Table I. DSC Data of HF-PP/mEBHC Blends

HF-PP/mEBHC	ΔH_{PP} (J/g)	X_c (%)
100/0	47.64	22.8
95/5	50.70	25.5
90/10	48.87	26.0
80/20	49.11	29.4
70/30	51.06	34.9
0/100	–	–
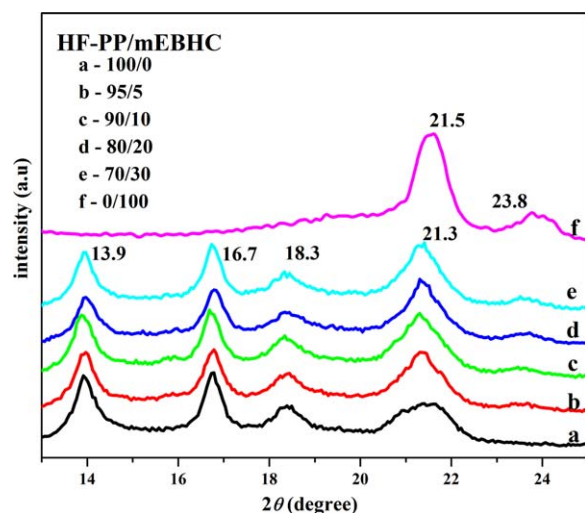
Figure 3. WAXD diffractograms of HF-PP/mEBHC blends. [Color figure can be viewed in the online issue, which is available at wileyonlinelibrary.com.]

evaluated from the variation of the full width at half-maximum (FWHM) of (1 1 0).[28] The values of FWHM decrease with the addition of mEBHC, which means that the packing coefficient of the macromolecules in the blends increases.[29] It can be concluded that mEBHC is an effective α-nucleating agent for heterogeneous nucleation of HF-PP, which is correlated with crystallinity increase of HF-PP/mEBHC blends at DSC section.

Fracture Surface Morphology. It is well known that the two-phase morphology of the polymer alloy has a dramatic effect on the properties and applications of the materials. Smaller size and more uniform distribution of the dispersed phase lead to the improvement of impact toughness of blend.[30] It is also helpful to predict the impact strength of the blends by examining their fractured surfaces. Usually, the rougher this fractured surface is, the more energy could be dissipated in an impact process and higher impact strength of the blend will be.[16] The SEM images of impact fractured surface of HF-PP/mEBHC blends are shown in Figure 4. The fracture surface of pristine HF-PP is rather smooth as shown in Figure 4(a). But for blends, the typical droplet-matrix micrographs are presented in the impact fractured surface as shown in Figure 4(b) and (c). One can observe that there are more droplets with better dispersion in fractured surface of HF-PP/mEBHC blends with 30 wt % mEBHC [Figure 4(b)] than the one with 10 wt % mEBHC [Figure 4(a)]. What is more, the fractured surfaces of HF-PP/mEBHC blends with 30 wt% mEBHC are rougher than that of 10 wt % mEBHC. Therefore, it could be predicted that HF-PP/mEBHC blends with 30 wt % mEBHC should have better impact strength than that with 10 wt % mEBHC.[16]

The mechanical properties, especially the impact toughness of polymer blends, rely heavily on their phase morphologies[31] and

Table II. The WAXD Data of HF-PP/mEBHC Blends

HF-PP/mEBHC	100/0	95/5	90/10	80/20	70/30
$I_{(110)}/I_{(040)}$	1.14	0.98	0.92	0.91	0.88
FWHM (110)	0.68	0.48	0.48	0.48	0.45
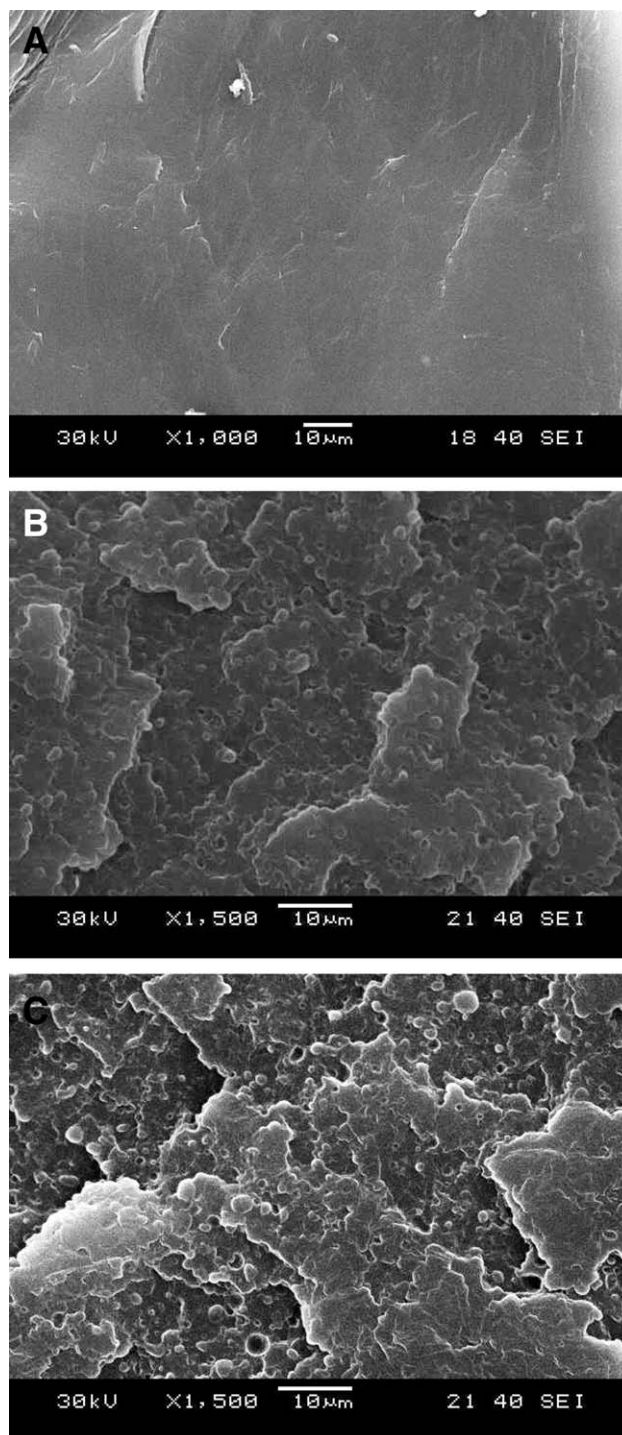
Figure 4. The SEM micrographs of fracture surface of HF-PP/mEBHC blends, (a) pristine HF-PP, (b) 10% mEBHC, and (c) 30% mEBHC.

are also closely related to their crystallinity.[2] Figure 5 shows the impact strength of HF-PP/mEBHC blends as a function of the incorporated mEBHC content at room temperature (23°C) and low temperature (−20°C). The curves show that the impact strength of HF-PP/mEBHC blends increases continuously with the increase of mEBHC. Compared to pristine HF-PP, the impact strength of the blends with 30% mEBHCC at 23°C and −20°C improved 150 and 35%, respectively. This significant improvement
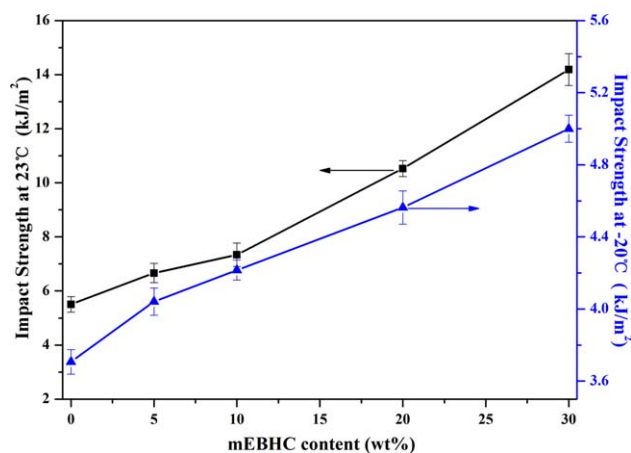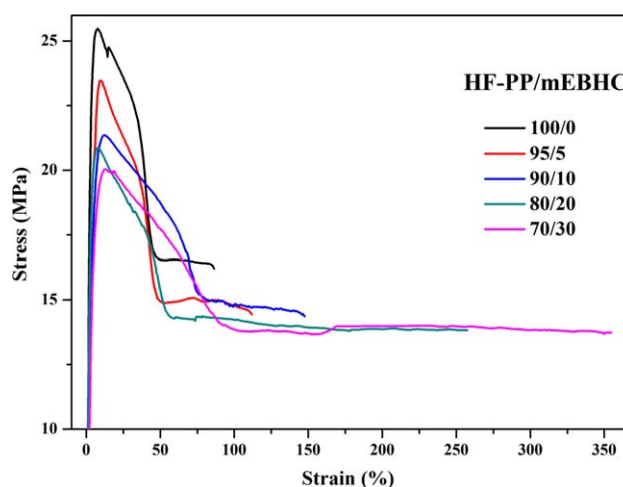
Figure 5. The impact strength of HF-PP with different mEBHC content at 23°C and −20°C.[Color figure can be viewed in the online issue, which is available at wileyonlinelibrary.com.]

Figure 6. The stress–strain curves of HF-PP/mEBHC blends with various mEBHC contents. [Color figure can be viewed in the online issue, which is available at wileyonlinelibrary.com.]

in impact strength of the blends could be ascribed to the higher crystallinity of HF-PP/mEBHC blends and the well-dispersed mEBHC particles in HF-PP matrix which has been revealed by SEM (Figure 4). Upon the impact, the flexible blocks of the mEBHC particles will first yield and deformed to absorb impact energy. And then further energy (or stress) dissipation will be transferred to the HF-PP continuous phase (especial crystalline region).[16] Therefore, the impact strength of HF-PP/mEBHC is significantly improved with the increase of the mEBHC content.

Stress–strain curves provide important information about yield strength and yield strain. Figure 6 shows the stress–strain curves of HF-PP/mEBHC blends. It is observed that all curves are shown as typical ductile plastic fracture behavior with a high yield stress and subsequent large strain. It is found that addition of mEBHC from 0 to 30 wt % gradually decreases the yield stress of blends. The elongation at break on the other hand increases significantly (from 87% to 379%) with the increasing mEBHC content. The tensile strength of blends only decrease from 25.4 ± 0.4 to 20.1 ± 0.4 MPa with a drop of 21% by adding 30 wt % of mEBHC (Table III). Moreover, the flexural properties of the blends are summarized in Table III. It can be seen that flexural properties including flexural module and flexural strength had a similar tendency as the tensile strength with drops of 19 and 17%, respectively. By incorporating mEBHC into HF-PP matrix, the stiffness including tensile and flexural properties decrease, which is similar to that of PP/toughen agent blends.[2,32,33]

Overall, toughness (impact strength), ductility (elongation at break) of HF-PP/mEBHC, were dramatically improved, while

the stiffness (tensile strength and flexural properties) was decreased with the incorporation of mEBHC.[34]

Rheology Properties of HF-PP/mEBHC Blends

The rheological properties of blends provide crucial guidance in optimizing the processing conditions of the blends.[34,35] The effects of shear rate on the viscosity of the blends were investigated at three different temperatures, 180, 200, and 220°C over a shear rate range of 300–5000 s^{-1}. As can be seen from Figure 7, the viscosities of both virgin polymers and all the blends decreased as the shear rate increased, indicating pseudoplastic behavior at 200°C. Similar behaviors were observed for the measurements at 180 and 220°C. It is worth noting that viscosity of pure mEBHC is about 131 Pa·s at 300 s^{-1} shear rate, which is lower than that of commonly used modifiers of PP impact strength such as mLLDPE (350 Pa·s)[36] and mEOC (910 Pa·s[2] and 230 Pa·s[13]). The viscosity of pure mEBHC is slightly higher than that of pristine HF-PP, and the viscosities of HF-PP/mEBHC blends are very close to that of pristine HF-PP. The viscosities of HF-PP/mEBHC blends with the high mEBHC content (80/20 and 70/30) were however slightly higher than that of pristine mEBHC at low shear rate. It is caused by the droplets-matrix morphology as mentioned in the "SEM" section. It has been seen from morphological data that more mEBHC content in the blend lead to higher droplet size in the morphology of fracture surfaces, which improves the viscosity of blends.[37] Above all, the incorporation of mEBHC would have minor influence on the viscosity of HFPP at high shear rate.

Table III. The Mechanical Properties of HF-PP/mEBHC Blends

Samples(HF-PP/mEBHC)	100/0	95/5	90/10	80/20	70/30
Tensile strength (MPa)	25.4 ± 0.4	23.4 ± 0.5	21.4 ± 0.5	20.2 ± 0.3	20.1 ± 0.4
Elongation at break (%)	87 ± 20	116 ± 16	147 ± 32	256 ± 27	379 ± 39
Flexural strength (MPa)	34.3 ± 0.4	32.2 ± 0.3	31.5 ± 0.4	28.8 ± 0.4	27.8 ± 0.2
Flexural modules (MPa)	1273 ± 38	1204 ± 27	1163 ± 25	1078 ± 34	1060 ± 19
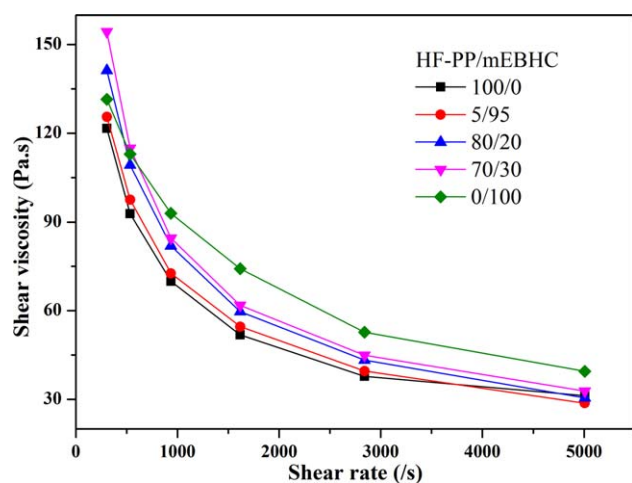
Figure 7. Plots of apparent shear viscosity versus shear rate for HF-PP/mEBHC blends at 200°C. [Color figure can be viewed in the online issue, which is available at wileyonlinelibrary.com.]

CONCLUSIONS

The mEBHC toughened HF-PP was prepared by mechanical blending and then melts extrusion. The crystallization, fracture morphology, rheological properties and mechanical properties of HF-PP/mEBHC were investigated. DSC analysis revealed that the phase separation of HF-PP/mEBHC blends occurred during cooling process. And, the incorporated mEBHC acted as a nucleation agent in the crystallization of HF-PP, causing a rise of crystallinity in HF-PP. The crystal structure of HF-PP was not affected by blending with mEBHC. The fracture surface morphology of the blends had the droplet-matrix structure. And the fractured surface of HF-PP/mEBHC blends became rougher by adding more mEBHC content as demonstrated in the SEM images. When mEBHC content increased from 0% to 30%, the impact strength at 23°C of HF-PP/mEBHC blends increased from 5.5 to 14.2 kJ/m^2 with a 150% increment. Meanwhile, the impact strength at −20°C of HF-PP/mEBHC blends had a continuous increase, and achieved 35% increment at 30 wt % mEBHC content. With the incorporation of mEBHC, the ductility of HF-PP was improved. But the tensile strength and flexural strength were slightly decreased. Compared with pristine HF-PP, the shear viscosities of blends had barely any change with adding mEBHC.

REFERENCES

1. Aboulkas, A.; El Harfi, K.; El Bouadili, A.; *Energy Conv. Manag.* **2010**, *51*, 1363.

2. Tang, W. H.; Tang, J.; Yuan, H. L.; Jin, R. G. *J. Appl. Polym. Sci.* **2011**, *122*, 461.

3. Premphet, K.; Paecharoenchai, W. *J. Appl. Polym. Sci.* **2002**, *85*, 2412.

4. Liang, J. Z.; Tang, C. Y.; Man, H. C. *J. Mater. Process. Technol.* **1997**, *66*, 158.

5. Ozcalik, O.; Tihminlioglu, F. *J. Food Eng.* **2013**, *114*, 505.

6. Sinha Ray, S.; Okamoto, M. *Prog. Polym. Sci.* **2003**, *28*, 1539.

7. Hussain, F.; Hojjati, M.; Okamoto, M.; Gorga, R. E. *J. Compos. Mater.* **2006**, *40*, 1511.

8. Jiang, Q.; Jia, H. B.; Wang, J. Y.; Fang, E. Y.; Jiang, J. *Iran. Polym. J.* **2012**, *21*, 201.

9. Ryu, S. H.; Gogos, C. G.; Xanthos, M. *Polymer*, **1991**, *32*, 2449.

10. Paul, B. K.; Paulo, B.-R. L.; Ahmedbhai, M. S.; J, R. D.; M, D. M. US Pat. 2,002,161,139 A1, **2002**−10−31.

11. Michael, Z. US Pat. 2,010,324,225,2010-12-23.

12. Ma, C. G.; Mai, Y. L.; Rong, M. Z.; Ruan, W. H.; Zhang, M. Q. *Compos. Sci. Technol.* **2007**, *67*, 2997.

13. McNally, T.; McShane, P.; Nally, G. M.; Murphy, W. R.; Cook, M.; Miller, A. *Polymer*, **2002**, *43*, 3785.

14. Wang, R; Li, G. X.; Yang, Q. *Plast. Rubber Compos.* **2007**, *36*, 314.

15. Premphet, K.; Horanont, P. *Polym. Plast. Technol. Eng.* **2001**, *40*, 235.

16. Liang, J. Z. *J. Polym. Environ.* **2012**, *20*, 872.

17. Wang, J.; Niu, H.; Dong, J.; Du, J.; Han, C. C. *Polymer* **2012**, *53*, 1507.

18. Wu, H.; Guo, S. Y. *Chinese J. Polym. Sci.* **2007**, *25*, 357.

19. Kukaleva, N.; Cser, F.; Jollands, M.; Kosior, E. *J. Appl. Polym. Sci.* **2000**, *77*, 1591.

20. Chen, X.; Zhang, S.; Xu, G.; Zhu, X.; Liu, W. *J. Appl. Polym. Sci.* **2012**, *125*, 1166.

21. Ghahri, S.; Najafi, S. K.; Mohebby, B.; Tajvidi, M. *J. Appl. Polym. Sci.* **2012**, *124*, 1074.

22. Wu, T.; Li, Y.; Wu, G. *Polymer*, **2005**, *46*, 3472.

23. Datta, N. K.; Birley, A. W. *Plast. Rubber Process. Appl.* **1982**, *2*, 237.

24. Li, X.; Wu, H.; Chen, J.; Yang, J.; Huang, T.; Zhang, N.; Wang, Y. *J. Appl. Polym. Sci.* **2012**, *126*, 1031.

25. Wang, S.; Zhang, J.; Chen, S.; Zhu, H. *J. Cryst. Growth* **2012**, *355*, 151.

26. Hojabri, L.; Jose, J.; Leao, A. L.; Bouzidi, L.; Narine, S. S. *Polymer* **2012**, *53*, 3762.

27. Rybnikář, F. *J. Appl. Polym. Sci.* **1989**, *38*, 1479.

28. Minardi, A.; Boudeulle, M.; Duval, E.; Etienne, S. *Polymer* **1997**, *38*, 3957.

29. Xu, T.; Lei, H.; Xie, C. S. *Mater. Design.* **2003**, *24*, 227.

30. Liu, Z. H.; Zhang, X. D.; Zhu, X. G.; Qi, Z. N.; Wang, F. S. *Polymer* **1997**, *38*, 5267.

31. Li, K.; Huang, H.-X. *Polym. Eng. Sci.* **2012**, *52*, 2157.

32. Abreu, F. O. M. S.; Forte, M. M. C.; Liberman, S. A. *J. Appl. Polym. Sci.* **2005**, *95*, 254.

33. Montfort, J. P.; Marin, G.; Arman, J.; Monge, P. *Polymer* **1978**, *19*, 277.

34. Lee, S. H.; Bailly, M.; Kontopoulou, M. *Macromol. Mater. Eng.* **2012**, *297*, 95.

35. Qin, S.-H.; Liu, H.; Zhang, M.-M.; He, M.; Yu, J. *Polym. Plast. Technol. Eng.* **2012**, *51*, 867.

36. Liu, C.; Wang, J.; He, J. *Polymer* **2002**, *43*, 3811.

37. Jafari, S.-H.; Hesabi, M.-N.; Khonakdar, H.; Asl-Rahimi, M. *J. Polym. Res.* **2011**, *18*, 821.